



ELSEVIER

Applied Acoustics 62 (2001) 289–305

**applied
acoustics**

www.elsevier.com/locate/apacoust

Natural frequencies of edge restrained tapered isotropic and orthotropic rectangular plates with a central free hole

Liz Graciela Nallim, Ricardo Oscar Grossi *

Facultad De Ingenieria Universidad Nacional De Salta, Avenida Bolivia 5150, 4400 Salta, Argentina

Received 7 September 1999; received in revised form 5 March 2000; accepted 30 March 2000

Abstract

Natural frequencies of tapered orthotropic rectangular plates with a central free hole and edges restrained against rotation and translation are studied by using orthogonal polynomials in the Rayleigh–Ritz method and applying a generalization of the Rayleigh–Schmidt method. The two methods are quite general and can be used to study plates with any combinations of boundary conditions, taper and geometric parameters. To demonstrate the accuracy of the present approach natural frequency coefficients are given for isotropic plates with a central free hole, from which comparison results are available. New results are also given for orthotropic plates with several complicating effects. The studied problems are of interest in several field of engineering, since holes are present in plates due to operational conditions. © 2001 Elsevier Science Ltd. All rights reserved.

1. Introduction

The determination of natural frequencies in transverse vibration of uniform thickness isotropic rectangular plates with complicating effects, such as elastically restrained edges and presence of holes with free edges, is a problem that has been extensively studied by several researches [1–6]. There is a comparatively limited amount of information on the vibration of isotropic and orthotropic plates with variable thickness and internal holes.

* Corresponding author. Fax: + 54-387-4255351.

E-mail address: promas@unsa.edu.ar or promas@ciunsa.edu.ar (R.O. Grossi).

The present paper deals with the determination of natural frequencies of rectangular isotropic and orthotropic plates with thickness variation, elastically restrained edges and a central rectangular free hole.

Frequency coefficients and eigenfunctions are obtained for different aspect ratios using several terms in the assumed shape function, when using the Ritz method along with orthogonal polynomials. On the other hand the fundamental frequency coefficient is obtained by using the Rayleigh–Schmidt method with various co-ordinate functions containing optimization parameters. It is the purpose of the present paper to present some technically interesting results for the natural frequencies of rectangular plates having an internal hole, since these are present in plates due to operational conditions, namely passage of conduits or ducts, electric conductors, and also constitute common structures used in naval as well as in ocean engineering.

2. Analysis

The maximum kinetic energy of the plate freely vibrating with amplitude $W(\hat{x}, \hat{y})$ and radian frequency ω is given by:

$$T_{\max} = \frac{\rho\omega^2}{2} \iint_R h(\hat{x}, \hat{y})W^2(\hat{x}, \hat{y})d\hat{x}d\hat{y} \tag{1}$$

where ρ is the mass density of the plate material, $h(\hat{x}, \hat{y})$ is the non-uniform plate thickness and the integration is carried out over the entire plate domain R . In the present study, the variation of thickness has been taken into account considering linear variation in \hat{x} and \hat{y} directions. The function that represents this variation is given by:

$$h = h(\hat{x}, \hat{y}) = h^{(1)}f(\hat{x})g(\hat{y}) \tag{2}$$

$$f(\hat{x}) = \left(1 + c_1 \frac{\hat{x}}{a}\right) \quad g(\hat{y}) = \left(1 + c_2 \frac{\hat{y}}{b}\right) \tag{3}$$

where $h^{(1)}$ is the value of h referred to edge 1, a and b are the side lengths of the plate in the \hat{x} and \hat{y} directions and c_1, c_2 are the taper parameters (see Fig. 1). The maximum strain energy of the mechanical system is given by:

$$U_{\max} = U_{p,\max} + U_{r,\max} + U_{t,\max} \tag{4}$$

$U_{p,\max}$ is the strain energy due to plate bending and is given by:

$$U_{p,\max} = \frac{1}{2} \iint_R \left[D_x(W_{\hat{x}\hat{x}})^2 + D_y(W_{\hat{y}\hat{y}})^2 + 2\mu_y D_x W_{\hat{x}\hat{x}} W_{\hat{y}\hat{y}} + 4D_{xy}(W_{\hat{x}\hat{y}})^2 \right] d\hat{x}d\hat{y} \tag{5}$$

where D_x and D_y are the flexural rigidities, D_{xy} is the torsional rigidity and they are given by

$$D_x(\hat{x}, \hat{y}) = D_x^{(1)} f^3(\hat{x}) g^3(\hat{y}), \quad D_x^{(1)} = \frac{E_x (h^{(1)})^3}{12(1 - \mu_x \mu_y)}$$

$$D_y(\hat{x}, \hat{y}) = D_y^{(1)} f^3(\hat{x}) g^3(\hat{y}), \quad D_y^{(1)} = \frac{E_y (h^{(1)})^3}{12(1 - \mu_x \mu_y)}$$

$$D_x^{(2)} = D_x^{(1)} f^3(a) g^3(b) = D_x^{(1)} C, \quad D_y^{(2)} = D_y^{(1)} f^3(a) g^3(b) = D_y^{(1)} C, \quad C = (1 + c_1)^3 (1 + c_2)^3$$

$$D_{xy}(\hat{x}, \hat{y}) = D_{xy}^{(1)} f^3(\hat{x}) g^3(\hat{y}), \quad D_{xy}^{(1)} = \frac{G_{xy} (h^{(1)})^3}{12}$$

where E_x and E_y are the Young's moduli in the \hat{x} and \hat{y} directions respectively, G_{xy} is the shear modulus and μ_x, μ_y are the Poisson's ratios.

The maximum strain energy stored in rotational and translational springs at the plate edges are, respectively:

$$U_{r,max} = \frac{1}{2} \left[r_1 \int_0^b (W_{\hat{x}}(0, \hat{y}))^2 d\hat{y} + r_2 \int_0^b (W_{\hat{x}}(a, \hat{y}))^2 d\hat{y} \right. \\ \left. + r_3 \int_0^a (W_{\hat{y}}(\hat{x}, 0))^2 d\hat{x} + r_4 \int_0^a (W_{\hat{y}}(\hat{x}, b))^2 d\hat{x} \right] \tag{6}$$

and

$$U_{t,max} = \frac{1}{2} \left[t_1 \int_0^b (W(0, \hat{y}))^2 d\hat{y} + t_2 \int_0^b (W(a, \hat{y}))^2 d\hat{y} \right. \\ \left. + t_3 \int_0^a (W(\hat{x}, 0))^2 d\hat{x} + t_4 \int_0^a (W(\hat{x}, b))^2 d\hat{x} \right] \tag{7}$$

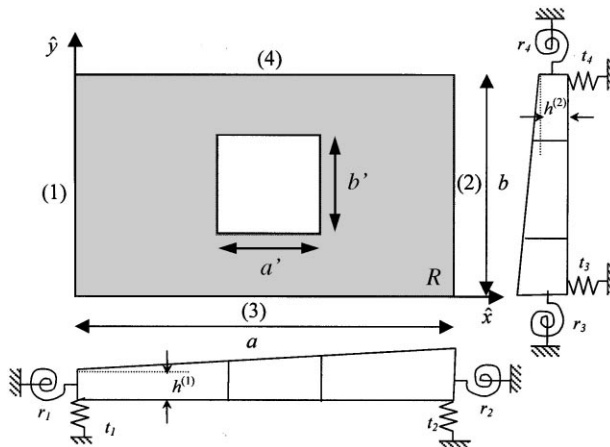


Fig. 1. The mechanical system investigated in the present study.

The constants r_i and t_i ($i=1,\dots,4$) are, respectively, the rotational and translational spring parameters along the corresponding edges. In the case of the mechanical system shown in Fig. 1, the governing boundary conditions which correspond to the external boundary of the plate are given by:

$$\left. \begin{aligned} r_1 W_{\hat{x}} &= D_x(W_{\hat{x}\hat{x}} + \mu_y W_{\hat{y}\hat{y}}) \\ t_1 W &= -[D_x W_{\hat{x}\hat{x}\hat{x}} + (4D_{xy} + \mu_y D_x)W_{\hat{x}\hat{y}\hat{y}}] \end{aligned} \right\} (\hat{x} = 0) \tag{8a}$$

$$\left. \begin{aligned} r_2 W_{\hat{x}} &= -D_x(W_{\hat{x}\hat{x}} + \mu_y W_{\hat{y}\hat{y}}) \\ t_2 W &= D_x W_{\hat{x}\hat{x}\hat{x}} + (4D_{xy} + \mu_y D_x)W_{\hat{x}\hat{y}\hat{y}} \end{aligned} \right\} (\hat{x} = a) \tag{8b}$$

$$\left. \begin{aligned} r_3 W_{\hat{y}} &= D_y(W_{\hat{y}\hat{y}} + \mu_x W_{\hat{x}\hat{x}}) \\ t_3 W &= -[D_y W_{\hat{y}\hat{y}\hat{y}} + (4D_{xy} + \mu_x D_y)W_{\hat{x}\hat{x}\hat{y}}] \end{aligned} \right\} (\hat{y} = 0) \tag{8c}$$

$$\left. \begin{aligned} r_4 W_{\hat{y}} &= -D_y(W_{\hat{y}\hat{y}} + \mu_x W_{\hat{x}\hat{x}}) \\ t_4 W &= D_y W_{\hat{y}\hat{y}\hat{y}} + (4D_{xy} + \mu_x D_y)W_{\hat{x}\hat{x}\hat{y}} \end{aligned} \right\} (\hat{y} = b) \tag{8d}$$

On the other hand the boundary conditions which correspond to the central free hole makes the exact treatment of the problem exceedingly complicated, since it is extremely difficult, if not impossible, to obtain co-ordinate functions which satisfy, identically, all the boundary conditions. But, as it is well known it is not necessary to subject the co-ordinate function to the natural boundary conditions. It is sufficient that they satisfy the geometric ones since as the number of co-ordinate functions approaches infinity, the natural boundary conditions will be exactly satisfied [7]. Consequently, when using the Rayleigh–Ritz method with a complete set of trial functions it is possible to ignore the natural boundary conditions in (8) and all the boundary conditions, which correspond to the free hole. On the other hand, in the application of the Rayleigh–Schmidt method, since only a few number of co-ordinate functions are used, it is convenient to replace the original natural boundary conditions by the following more easily applied conditions:

$$\left. \begin{aligned} R_1 W_x &= W_{xx} \\ T_1 W &= -W_{xxx} \end{aligned} \right\} (x = 0) \tag{9a}$$

$$\left. \begin{aligned} R_2 W_x &= -W_{xx} \\ T_2 W &= W_{xxx} \end{aligned} \right\} (x = 1) \tag{9b}$$

$$\left. \begin{aligned} R_3 W_y &= W_{yy} \\ T_3 W &= -W_{yyy} \end{aligned} \right\} (y = 0) \tag{9c}$$

$$\left. \begin{aligned} R_4 W_y &= -W_{yy} \\ T_4 W &= W_{yyy} \end{aligned} \right\} (y = 1) \tag{9d}$$

where

$$R_1 = \frac{r_1 a}{D_x^{(1)}}, \quad T_1 = \frac{t_1 a^3}{D_x^{(1)}}, \quad R_2 = \frac{r_2 a}{D_x^{(2)}}, \quad T_2 = \frac{t_2 a^3}{D_x^{(2)}}$$

$$R_3 = \frac{r_3 b}{D_y^{(1)}}, \quad T_3 = \frac{t_3 b^3}{D_y^{(1)}}, \quad R_4 = \frac{r_4 b}{D_y^{(2)}}, \quad T_4 = \frac{t_4 b^3}{D_y^{(2)}}$$

The change of variables $x = \hat{x}/a$ and $y = \hat{y}/b$ has been used in Eq. (9) and will be used in the following in order to work in more adequate intervals of integration.

3. The Rayleigh–Ritz method

The assumed shape function for using the Rayleigh–Ritz procedure are given by

$$\left[W(x, y) = \sum_i \sum_j c_{ij} p_i(x) q_j(y) \right] \tag{10}$$

where $p_i(x)$ and $q_j(y)$ are the orthogonal polynomials, and c_{ij} are the arbitrary coefficients which are to be determined. The procedure for the construction of the orthogonal polynomials has been developed by Bhat [8,9]. A brief description of the procedure to obtain the set of orthogonal polynomials is given here.

The first member of the set, $p_1(x)$ is obtained as the simplest polynomial that satisfies the geometrical boundary conditions. Assume

$$\left[p_1(x) = \sum_{i=1}^5 a_i x^{i-1} \right] \tag{11}$$

The arbitrary constants, a_i are determined by substituting Eq. (11) in the mentioned boundary conditions. The higher members of the set are obtained employing the Gram–Schmidt orthogonalization procedure as

$$\left[\begin{aligned} p_2(x) &= (x - B_2)p_1(x) \\ p_k(x) &= (x - B_k)p_{k-1}(x) - C_k p_{k-2}(x) \end{aligned} \right] \tag{12}$$

where $B_k = \frac{\int_0^1 \eta(x) x (p_{k-1}(x))^2 dx}{\int_0^1 \eta(x) (p_{k-1}(x))^2 dx}$, $C_k = \frac{\int_0^1 \eta(x) x p_{k-1}(x) p_{k-2}(x) dx}{\int_0^1 \eta(x) (p_{k-2}(x))^2 dx}$

where $\eta(x)$ is a weight function used in the orthogonalization. For tapered plates with thickness varying as Eq.(2), $\eta(x)$ can be taken as $h(x)$ itself.

The polynomials set along the y direction is also generated using the same procedure. The natural frequencies are obtained from the Rayleigh quotient as:

$$\left[\omega^2 = \frac{U_{\max}}{T_{\max}} \right] \tag{13}$$

Minimization of the Rayleigh quotient (13) with respect to each parameter c_{ij} , leads to the necessary conditions

$$\left[\frac{\partial \omega^2}{\partial c_{ij}} = 0 \right] \tag{14}$$

Substituting the approximate function (10) into Eq.(14) one obtains:

$$\left[\sum_i \sum_j [K_{ijkh} - \Omega^2 M_{ijkh}] c_{ij} = 0 \right] \tag{15}$$

where $\Omega = \sqrt{\frac{\rho h^{(1)}}{H_{xy}^{(1)}}} \omega a^2$ is the non-dimensional frequency parameter and

$$\begin{aligned} H_{xy}^{(1)} &= \mu_y D_x^{(1)} + 2D_{xy}^{(1)} \\ K_{ijkh} &= \frac{D_x^{(1)}}{H_{xy}^{(1)}} \left(\sum_{r=1}^4 P_{x_{ik}^{1,r}} P_{y_{jh}^{1,r}} \right) + \frac{D_y^{(1)}}{H_{xy}^{(1)}} r_\ell^4 \left(\sum_{r=1}^4 P_{x_{ik}^{2,r}} P_{y_{jh}^{2,r}} \right) \\ &\quad + \mu_y \frac{D_x^{(1)}}{H_{xy}^{(1)}} r_\ell^2 \left[\sum_{r=1}^4 \left(P_{x_{ik}^{31,r}} P_{y_{jh}^{31,r}} + P_{x_{ik}^{32,r}} P_{y_{jh}^{32,r}} \right) \right] + 4 \frac{D_{xy}^{(1)}}{H_{xy}^{(1)}} r_\ell^2 \left(\sum_{r=1}^4 P_{x_{ik}^{4,r}} P_{y_{jh}^{4,r}} \right) \\ &\quad + \frac{D_x^{(1)}}{H_{xy}^{(1)}} R_1 R_{x_{ik}^1} R_{y_{jh}^1} + \frac{D_x^{(1)}}{H_{xy}^{(1)}} C R_2 R_{x_{ik}^2} R_{y_{jh}^2} + \frac{D_y^{(1)}}{H_{xy}^{(1)}} r_\ell^4 R_3 R_{x_{ik}^3} R_{y_{jh}^3} \\ &\quad + \frac{D_y^{(1)}}{H_{xy}^{(1)}} r_\ell^4 C R_4 R_{x_{ik}^4} R_{y_{jh}^4} + \frac{D_x^{(1)}}{H_{xy}^{(1)}} T_1 T_{x_{ik}^1} T_{y_{jh}^1} + \frac{D_x^{(1)}}{H_{xy}^{(1)}} C T_2 T_{x_{ik}^2} T_{y_{jh}^2} \\ &\quad + \frac{D_y^{(1)}}{H_{xy}^{(1)}} r_\ell^4 T_3 T_{x_{ik}^3} T_{y_{jh}^3} + \frac{D_y^{(1)}}{H_{xy}^{(1)}} r_\ell^4 C T_4 T_{x_{ik}^4} T_{y_{jh}^4} \\ M_{ijkh} &= \sum_{r=1}^4 C x_{ik}^r C y_{jh}^r, \quad r_\ell = \frac{a}{b} \end{aligned}$$

The analytical expressions of the terms $P_{x_{ik}^{1,r}}, P_{x_{ik}^{2,r}}, P_{x_{ik}^{31,r}}, P_{x_{ik}^{32,r}}, P_{x_{ik}^{4,r}}, R_{x_{ik}^r}, T_{x_{ik}^r}, C x_{ik}^r, P_{y_{jh}^{1,r}}, P_{y_{jh}^{2,r}}, P_{y_{jh}^{31,r}}, P_{y_{jh}^{32,r}}, P_{y_{jh}^{4,r}}, R_{y_{jh}^r}, T_{y_{jh}^r}, C y_{jh}^r$ ($r = 1, \dots, 4$) are given in the Appendix A.

4. The generalized Rayleigh–Schmidt method

The assumed shape function for using the generalized Rayleigh–Schmidt method comprising several adjustable exponents is expressed in the form:

$$\left[W(x, y) = \sum_{i=1}^N A_i X_i(x) Y_i(y) \right] \tag{16}$$

$$\left[X_i(x) = \sum_{j=0}^{i+3} a_{i,j} x^{n_{i,j}}, \quad Y_i(y) = \sum_{j=0}^{i+3} b_{i,j} y^{n_{i,j}} \right]$$

where $a_{i,j} = b_{i,j} = 1, i = 1, \dots, N, j = 4, \dots, i + 3$, (the other coefficients $a_{i,j}$ and $b_{i,j}$ are determined from the approximate boundary conditions (9), $n_{i,j} = j, i = 1, \dots, N, j = 0, \dots, i + 2$ and $n_{i,i+3}$ are the adjustable exponents.

Minimization of the Rayleigh quotient (13) with respect to each parameter A_i , leads to the necessary conditions: $\frac{\partial \omega^2}{\partial A_i} = 0, \quad i = 1, \dots, N$

This results in the follow eigenvalue problem

$$[[K] - \Omega^2[M] = 0] \tag{17}$$

where:

$$\begin{aligned} K_{kl} = & \frac{D_x^{(1)}}{H_{xy}^{(1)}} \sum_{r=1}^4 P x_{kl}^{1,r} P y_{kl}^{1,r} + \frac{D_y^{(1)}}{H_{xy}^{(1)}} r_\ell^4 \sum_{r=1}^4 P x_{kl}^{2,r} P y_{kl}^{2,r} \\ & + \mu_y \frac{D_x^{(1)}}{H_{xy}^{(1)}} r_\ell^2 \sum_{r=1}^4 (P x_{kl}^{31,r} P y_{kl}^{31,r} + P x_{kl}^{32,r} P y_{kl}^{32,r}) + 4 \frac{D_{xy}^{(1)}}{H_{xy}^{(1)}} r_\ell^2 \sum_{r=1}^4 P x_{kl}^{4,r} P y_{kl}^{4,r} \\ & + R_1 \frac{D_x^{(1)}}{H_{xy}^{(1)}} R x_{kl}^1 R y_{kl}^1 + \frac{D_x^{(1)}}{H_{xy}^{(1)}} C R_2 R x_{kl}^2 R y_{kl}^2 + \frac{D_y^{(1)}}{H_{xy}^{(1)}} r_\ell^4 R_3 R x_{kl}^3 R y_{kl}^3 \\ & + \frac{D_y^{(1)}}{H_{xy}^{(1)}} r_\ell^4 C R_4 R x_{kl}^4 + \frac{D_x^{(1)}}{H_{xy}^{(1)}} T_1 T x_{kl}^1 T y_{kl}^1 + \frac{D_x^{(1)}}{H_{xy}^{(1)}} C T_2 T x_{kl}^2 T y_{kl}^2 \\ & + \frac{D_y^{(1)}}{H_{xy}^{(1)}} r_\ell^4 T_3 T x_{kl}^3 T y_{kl}^3 + \frac{D_y^{(1)}}{H_{xy}^{(1)}} r_\ell^4 C T_4 T x_{kl}^4 T y_{kl}^4 \\ M_{kl} = & \sum_{r=1}^4 C x_{kl}^r C y_{kl}^r \end{aligned}$$

The analytical expressions of the terms $P x_{kl}^{1,r}, P x_{kl}^{2,r}, P x_{kl}^{31,r}, P x_{kl}^{32,r}, P x_{kl}^{4,r}, R x_{kl}^r, T x_{kl}^r, C x_{kl}^r, P y_{kl}^{1,r}, P y_{kl}^{2,r}, P y_{kl}^{31,r}, P y_{kl}^{32,r}, P y_{kl}^{4,r}, R y_{kl}^r, T y_{kl}^r, C y_{kl}^r (r = 1, \dots, 4)$ are given in the Appendix B.

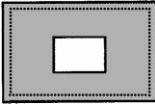
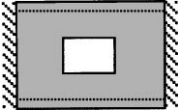
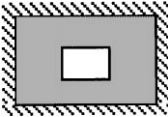
The corresponding fundamental frequency coefficient is a function of the parameters $n_{i,i+3}$, introduced in Eq. (16), therefore it can be written $\Omega_{11} = \Omega_{11}(n_{i,i+3})$. The Rayleigh- Schmidt procedure requires the minimization of this coefficient with respect to $n_{i,i+3}$. Obviously, the procedure of differentiation in Eq. (17), for the purpose of minimization is very difficult. Nevertheless the variation of the adjustable exponents parameter $n_{i,i+3}$ in a neighbourhood of the corresponding integer value $i + 3$ is sufficient to determine the approximate value for the minimum frequency coefficient.

5. Numerical results

A great number of problems were solved and since the number of cases is prohibitively large, results are presented for only a few cases. All calculations have been performed taking the Poisson ratios $\mu_y = 0.3$.

Table 1 depicts the fundamental and higher frequency coefficients in the case of a square plate of side a with concentric square perforations of side $a' = b'$, for three types of boundary conditions.

Table 1
Values of Ω_{11} , Ω_{12} , Ω_{22} with $\Omega_{ij} = \sqrt{\frac{\rho H^{(1)}}{H_{xy}^{(1)}} \omega_{ij} a^2}$ for a uniform square plate with a concentric square hole

	$r_a = \frac{a'}{a}$	$r_\ell = a/b = 1$									
		Ω_{11}				Ω_{12}			Ω_{22}		
		(I) ^a	(II) ^b	(III) ^c	(IV) ^d	(II)	(III)	(V) ^e	(II)	(III)	(V)
	$r_a = 0.1$	19.87	19.87	19.43	19.87	49.35	49.13	–	78.43	78.31	–
	$r_b = 0.1$										
	$r_a = 0.2$	20.20	20.19	19.11	20.19	49.39	47.78	–	77.47	76.02	–
	$r_b = 0.2$										
	$r_a = 0.3$	20.80	20.70	–	20.70	49.51	–	–	76.05	–	–
	$r_b = 0.3$										
	$r_a = 0.1$	29.27	29.27	28.69	–	54.75	54.53	55.13	93.92	93.83	94.41
	$r_b = 0.1$										
	$r_a = 0.2$	30.31	30.21	–	–	54.84	–	55.29	92.40	–	93.34
	$r_b = 0.2$										
	$r_a = 0.3$	32.49	32.19	31.09	–	55.04	49.13	55.86	91.30	88.26	92.71
	$r_b = 0.3$										
	$r_a = 0.1$	36.54	36.50	35.67	–	73.41	72.83	74.33	107.33	106.82	107.80
	$r_b = 0.1$										
	$r_a = 0.2$	38.34	38.11	36.67	–	73.63	69.90	74.73	105.47	104.15	106.46
	$r_b = 0.2$										
	$r_a = 0.3$	42.25	41.79	40.58	–	73.98	65.50	76.19	104.34	100.15	105.97
	$r_b = 0.3$										
	$r_a = 0.4$	50.28	49.90	49.13	–	74.75	65.92	80.57	105.04	99.19	108.67
	$r_b = 0.4$										

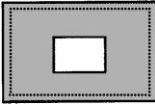
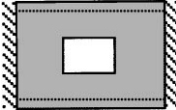
^a Rayleigh–Schmidt method.
^b Rayleigh–Ritz method.
^c Finite element solution.
^d Reference [3].
^e Reference [4].

Table 2 depicts the fundamental and higher frequency coefficients in the case of a rectangular plate with aspect ratio $r_\ell = a/b = 1.5$, for three types of boundary conditions.

Tables 1 and 2 both depict comparisons of frequency coefficients as obtained: (1) by means of the Rayleigh–Schmidt method and (2) by means of the Rayleigh–Ritz method with orthogonal polynomials. The frequency coefficients have been verified using a finite element algorithmic procedure and also compared with those available in the literature [3,4]. The agreement of results obtained with the Rayleigh–Ritz method and the F.E.M is adequate from engineering viewpoint. For the case of

Table 2

Values of Ω_{11} , Ω_{12} , Ω_{22} with $\Omega_{ij} = \sqrt{\frac{\rho H_{xy}^{(i)}}{H_{xy}^{(j)}} \omega_{ij} a^2}$ for a uniform isotropic rectangular plate with a concentric rectangular hole

$r_a = \frac{a'}{a}$ $r_b = \frac{b'}{b}$		$r_\ell = a/b = 1.5$									
		Ω_{11}				Ω_{12}			Ω_{22}		
		(I) ^a	(II) ^b	(III) ^c	(IV) ^d	(II)	(III)	(V) ^e	(II)	(III)	(V)
	$r_a = 0.1$ $r_b = 0.1$	31.88	32.25	–	32.25	98.72	–	–	112.7	–	–
	$r_a = 0.2$ $r_b = 0.2$	32.01	32.63	–	32.62	98.76	–	–	114.53	–	–
	$r_a = 0.3$ $r_b = 0.3$	33.23	33.12	–	33.11	98.59	–	–	124.26	–	–
	$r_a = 0.4$ $r_b = 0.4$	34.63	34.38	–	34.41	96.63	–	–	123.69	–	–
	$r_a = 0.1$ $r_b = 0.1$	39.60	39.60	38.42	–	102.25	101.01	103.3	138.81	137.85	139.7
	$r_a = 0.2$ $r_b = 0.2$	41.47	40.98	38.86	–	102.37	92.62	104.2	136.15	133.15	137.6
	$r_a = 0.3$ $r_b = 0.3$	45.61	44.58	43.00	–	100.55	84.00	107.6	135.04	128.05	137.9
	$r_a = 0.4$ $r_b = 0.4$	54.84	53.73	52.54	–	98.39	86.15	115.4	136.66	128.76	143.7
	$r_a = 0.1$ $r_b = 0.1$	62.20	62.02	60.55	–	148.88	146.46	151.6	177.91	148.32	179.6
	$r_a = 0.2$ $r_b = 0.2$	67.10	66.41	64.73	–	149.33	135.46	154.2	175.20	156.23	177.6
	$r_a = 0.3$ $r_b = 0.3$	79.12	77.46	75.84	–	151.04	139.49	165.2	175.34	168.59	179.7
	$r_a = 0.4$ $r_b = 0.4$	–	90.82	86.47	–	174.59	172.31	198.0	181.04	177.53	191.2

^a Rayleigh–Schmidt method.

^b Rayleigh–Ritz method.

^c Finite element solution.

^d Reference [3].

^e Reference [4].

square plate (shown in Table 1) the maximum differences are of the order of 3%. In the case of a rectangular plate, depicted in Table 2, the maximum differences are of the order of 5%. The numbers of mesh elements used are 40×40 in Table 1 and 40×60 in Table 2. The values obtained with the Rayleigh–Schmidt method are less accurate with respect to the values obtained with a Rayleigh–Ritz method in almost all cases.

On the other hand, the eigenvalues determined in reference [4] constitute, in some cases, extremely high upper bounds (in general they are rather high upper bounds but a single term polynomial approximation was used in that study).

Table 3 depicts values of the first five modes frequency coefficients Ω_i , with $\Omega_i = \sqrt{\frac{\rho h^{(1)}}{H_{xy}^{(1)}} \omega_i a^2}$, ($i = 1, \dots, 5$) obtained by the application of the Rayleigh–Ritz method with orthogonal polynomials, for the general case of a tapered orthotropic plate with elastically restrained ends and with a rectangular hole.

It is observed that for all the situations depicted for isotropic plates (Table 1 and Table 2), the values of the fundamental frequency increases with respect to the well-known values of the fundamental frequency of the solid plate. This effect is defined as ‘dynamic stiffening’ [5]. In the general case of a tapered orthotropic plate with a concentric hole, the dynamic stiffening can also be observed (see Fig. 2). It

Table 3

Values of Ω_i with $\Omega_i = \sqrt{\frac{\rho h^{(1)}}{H_{xy}^{(1)}} \omega_i a^2}$, $i = 1, \dots, 5$, for a tapered orthotropic rectangular plate with a concentric rectangular hole and with rotational restraint R_2 and translational restraint T_2

		$R_2 = 10 \quad T_2 = 100$								
		$r_\ell = a/b$	$r_a = a'/a$	$r_b = b'/b$	Ω_1	Ω_2	Ω_3	Ω_4	Ω_5	
$c_1 = 0$	$c_2 = 0$	0.5	0.1	0.1	10.492	13.549	21.273	24.120	29.726	
			0.2	0.2	10.575	13.841	21.211	24.188	30.258	
$c_1 = -0.2$	$c_2 = 0.2$	1	0.3	0.3	10.696	14.383	21.251	24.401	30.680	
			0.1	0.2	11.847	26.513	27.803	48.810	54.408	
			0.1	0.3	11.872	26.495	27.905	49.030	54.355	
			0.2	0.3	11.926	26.350	28.392	50.093	54.299	
			0.2	0.1	14.819	30.971	54.232	59.250	78.311	
			0.2	0.2	14.834	30.995	54.334	59.122	79.092	
$c_1 = -0.2$	$c_2 = 0.2$	1.5	0.2	0.3	14.849	31.039	54.427	59.054	79.823	
			0.1	0.1	10.613	13.606	20.901	24.713	29.744	
			0.2	0.2	10.712	13.887	20.804	24.819	29.916	
			0.3	0.3	10.850	14.407	20.797	25.143	30.309	
			1	0.1	0.2	11.844	26.551	27.087	48.351	55.631
				0.1	0.3	11.868	26.479	27.237	48.607	55.601
				0.2	0.3	11.922	26.269	27.790	49.729	55.631
				0.2	0.1	14.410	30.861	50.671	59.914	76.968
			1.5	0.2	0.2	14.418	30.930	50.730	59.782	77.951
				0.2	0.3	14.427	30.019	50.798	59.661	78.956

^a ($R_1 = R_3 = T_1 = T_3 = \infty$, $R_4 = T_4 = 0$, $R_2 = \frac{r_2 a}{D_x^{(2)}}$, $T_2 = \frac{t_2 a^3}{D_x^{(2)}}$, $\frac{D_x^{(1)}}{H_{xy}^{(1)}} = 0.5$, $\frac{D_y^{(1)}}{H_{xy}^{(1)}} = 1$, $\mu_y = 0.3$).

seems reasonable to assume that the dynamic stiffening effect becomes noticeable for $r_a = r_b > 0.25$.

Figs. 3 and 4 show the variation of the square of the fundamental frequency coefficient (Ω_{11}^2) with the orthotropic parameters ($D_x^{(1)}/H_{xy}^{(1)}$) and ($D_y^{(1)}/H_{xy}^{(1)}$), for a square tapered plate ($c_1 = 0.2, c_2 = -0.2$) having a central free hole ($r_a = r_b = 0.3$). In Fig. 3 the plate is simply supported and in Fig. 4 is clamped. It would appear from these figures that the variation in the square of the frequency with either

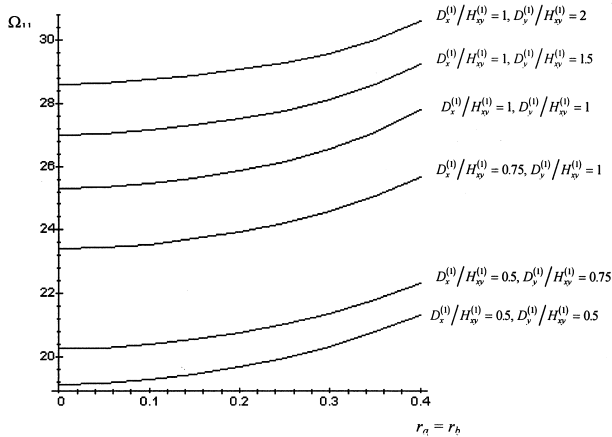


Fig. 2. Variation of fundamental frequency parameter Ω_{11} with perforation ratio $r_a = r_b$, of a square plate, for six different orthotropic parameters. Taper parameters: $c_1 = 0.2, c_2 = 0.4$. Boundary conditions: clamped on edge 1, simply supported on edges 3 and 4, elastically restrained on edge 2 ($T_2 = 50, R_2 = 10$).

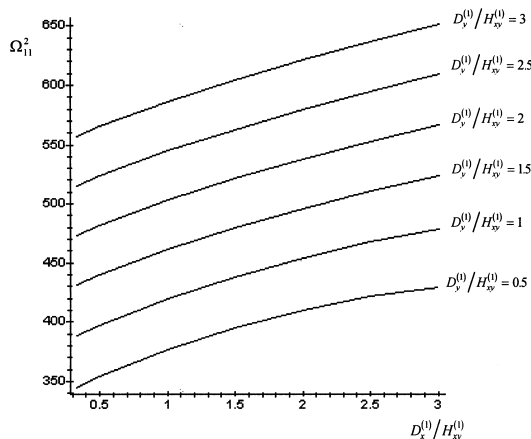


Fig. 3. Fundamental frequency parameters Ω_{11}^2 against $D_x^{(1)}/H_{xy}^{(1)}$ and $D_y^{(1)}/H_{xy}^{(1)}$ for a simply supported tapered ($c_1 = 0.2, c_2 = -0.2$) orthotropic square plate, having a central free hole ($r_a = r_b = 0.3$).

$(D_x^{(1)}/H_{xy}^{(1)})$ or $(D_y^{(1)}/H_{xy}^{(1)})$ is linear in almost all cases, with the slopes on Fig. 4 greater than those on Fig. 3. These slope variations can also be observed in Fig. 5, in which the square of the fundamental frequency parameter (Ω_{11}^2) for a square tapered plate ($c_1 = 0.2, c_2 = -0.2$) having a central free hole ($r_a = r_b = 0.3$), is plotted against the orthotropic parameter ($D_x^{(1)}/H_{xy}^{(1)}$) for several values of the rotational restraints ($R_1 = R_2 = R_3 = R_4$) and for $(D_y^{(1)}/H_{xy}^{(1)}) = 1.5$. It's interesting to point out that the curve slope increases as R_i increases.

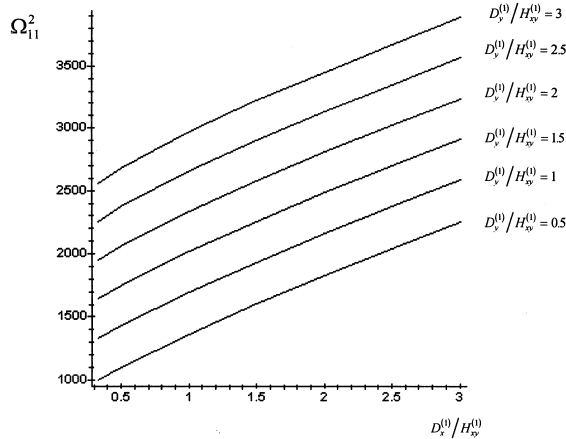


Fig. 4. Fundamental frequency parameters Ω_{11}^2 against $D_x^{(1)}/H_{xy}^{(1)}$ and $D_y^{(1)}/H_{xy}^{(1)}$ for a clamped tapered ($c_1 = 0.2, c_2 = -0.2$) orthotropic square plate, having a central free hole ($r_a = r_b = 0.3$).

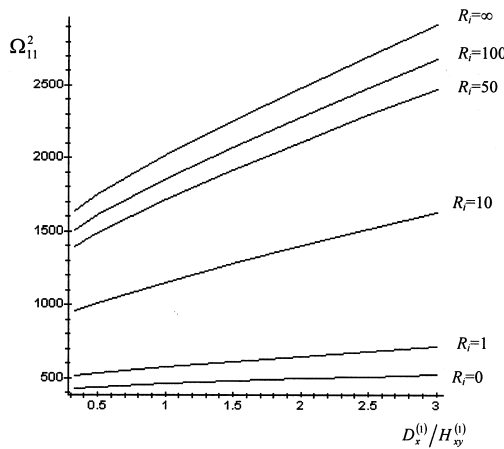


Fig. 5. Variation of fundamental parameters Ω_{11}^2 of a square tapered plate ($c_1 = 0.2, c_2 = -0.2$), having a central free hole ($r_a = r_b = 0.3$), with orthotropic parameter $D_x^{(1)}/H_{xy}^{(1)}$, for various values of rotational restraints parameters ($R_1 = R_2 = R_3 = R_4$). $D_y^{(1)}/H_{xy}^{(1)} = 1.5, T_i = \infty, i = 1, \dots, 4$.

6. Conclusions

The Rayleigh–Ritz and Rayleigh–Schmidt methods have been used to obtain computationally efficient and accurate approximate approaches in the determination of frequencies of free vibration of plates with a central free hole. The algorithms developed are very general and take into account a great variety of complicating effects, such as non-uniform cross sections, ends elastically restrained against rotation and translation. Several particular cases were solved and the results obtained were compared with previously published results to demonstrate the accuracy and flexibility of the present approaches. New results for tapered orthotropic plates with generally restrained ends and central holes were included.

The algorithms presented have a great flexibility and good accuracy and constitute an efficient tool for the rapid and inexpensive determination of natural frequencies in an important number of plate vibrating problems, being in consequence, of interest in design works.

Acknowledgements

The authors are indebted to the reviewers of the paper for their constructive comments and suggestions and to Dr. Patricio A. A. Laura and Dr. Bibiana Lucioni for their contributions. The present study has been sponsored by CONICET and Consejo de Investigación (UNSA).

Appendix A. Definitions of variables and parameters in Eq. (15)

$$r_a = \frac{a'}{a}, \quad r_b = \frac{b'}{b}$$

$$P_{ik}^{1,1} = \int_0^{\frac{1}{2}(1-r_a)} f^{\beta}(x) p_i'' p_k'' dx, \quad P_{ik}^{1,2} = \int_{\frac{1}{2}(1-r_a)}^{\frac{1}{2}(1+r_a)} f^{\beta}(x) p_i'' p_k'' dx,$$

$$P_{ik}^{1,3} = \int_{\frac{1}{2}(1+r_a)}^1 f^{\beta}(x) p_i'' p_k'' dx,$$

$$P_{ik}^{1,4} = P_{ik}^{1,2}, \quad P_{ik}^{2,1} = \int_0^{\frac{1}{2}(1-r_a)} f^{\beta}(x) p_i p_k dx, \quad P_{ik}^{2,2} = \int_{\frac{1}{2}(1-r_a)}^{\frac{1}{2}(1+r_a)} f^{\beta}(x) p_i p_k dx,$$

$$P_{ik}^{2,3} = \int_{\frac{1}{2}(1+r_a)}^1 f^{\beta}(x) p_i p_k dx, \quad P_{ik}^{2,4} = P_{ik}^{2,2}, \quad P_{ik}^{3,1} = \int_0^{\frac{1}{2}(1-r_a)} f^{\beta}(x) p_i'' p_k dx,$$

$$P_{ik}^{3,2} = \int_{\frac{1}{2}(1-r_a)}^{\frac{1}{2}(1+r_a)} f^{\beta}(x) p_i'' p_k dx, \quad P_{ik}^{3,3} = \int_{\frac{1}{2}(1+r_a)}^1 f^{\beta}(x) p_i'' p_k dx, \quad P_{ik}^{3,4} = P_{ik}^{3,2},$$

$$Px_{ik}^{32,1} = \int_0^{\frac{1}{2}(1-r_a)} f^3(x) p_i p_k'' dx, \quad Px_{ik}^{32,2} = \int_{\frac{1}{2}(1-r_a)}^{\frac{1}{2}(1+r_a)} f^3(x) p_i p_k'' dx,$$

$$Px_{ik}^{32,3} = \int_{\frac{1}{2}(1+r_a)}^1 f^3(x) p_i p_k'' dx$$

$$Px_{ik}^{32,4} = Px_{ik}^{32,2}, \quad Px_{ik}^{4,1} = \int_0^{\frac{1}{2}(1-r_a)} f^3(x) p_i' p_k' dx, \quad Px_{ik}^{4,2} = \int_{\frac{1}{2}(1-r_a)}^{\frac{1}{2}(1+r_a)} f^3(x) p_i' p_k' dx,$$

$$Px_{ik}^{4,3} = \int_{\frac{1}{2}(1+r_a)}^1 f^3(x) p_i' p_k' dx, \quad Px_{ik}^{4,4} = Px_{ik}^{4,2}$$

$$Rx_{ik}^1 = p_i'(0) p_k'(0), \quad Rx_{ik}^2 = p_i'(1) p_k'(1), \quad Rx_{ik}^3 = \int_0^1 p_i(x) p_k(x) dx, \quad Rx_{ik}^4 = Rx_{ik}^3$$

$$Tx_{ik}^1 = p_i(0) p_k(0), \quad Tx_{ik}^2 = p_i(1) p_k(1), \quad Tx_{ik}^3 = Rx_{ik}^3, \quad Tx_{ik}^4 = Tx_{ik}^3$$

$$Cx_{ik}^1 = \int_0^{\frac{1}{2}(1-r_a)} f(x) p_i p_k dx, \quad Cx_{ik}^2 = \int_{\frac{1}{2}(1-r_a)}^{\frac{1}{2}(1+r_a)} f(x) p_i p_k dx,$$

$$Cx_{ik}^3 = \int_{\frac{1}{2}(1+r_a)}^1 f(x) p_i p_k dx, \quad Cx_{ik}^4 = Cx_{ik}^2$$

$$Py_{jh}^{1,1} = \int_0^1 g^3(y) q_j q_h dy, \quad Py_{jh}^{1,2} = \int_0^{\frac{1}{2}(1-r_b)} g^3(y) q_j q_h dy, \quad Py_{jh}^{1,3} = Py_{jh}^{1,1}$$

$$Py_{jh}^{1,4} = \int_{\frac{1}{2}(1+r_b)}^1 g^3(y) q_j q_h dy, \quad Py_{jh}^{2,1} = \int_0^1 g^3(y) q_j' q_h'' dy, \quad Py_{jh}^{2,2} = \int_0^{\frac{1}{2}(1-r_b)} g^3(y) q_j' q_h'' dy$$

$$Py_{jh}^{2,3} = Py_{jh}^{2,1}, \quad Py_{jh}^{2,4} = \int_{\frac{1}{2}(1+r_b)}^1 g^3(y) q_j' q_h'' dy, \quad Py_{jh}^{3,1} = \int_0^1 g^3(y) q_j' q_h dy,$$

$$Py_{jh}^{3,2} = \int_0^{\frac{1}{2}(1-r_b)} g^3(y) q_j' q_h dy, \quad Py_{jh}^{3,3} = Py_{jh}^{3,1}, \quad Py_{jh}^{3,4} = \int_{\frac{1}{2}(1+r_b)}^1 g^3(y) q_j' q_h dy,$$

$$Py_{jh}^{32,1} = \int_0^1 g^3(y) q_j q_h'' dy, \quad Py_{jh}^{32,2} = \int_0^{\frac{1}{2}(1-r_b)} g^3(y) q_j q_h'' dy, \quad Py_{jh}^{32,3} = Py_{jh}^{32,1}$$

$$Py_{jh}^{32,4} = \int_{\frac{1}{2}(1+r_b)}^1 g^3(y) q_j q_h'' dy, \quad Py_{jh}^{4,1} = \int_0^1 g^3(y) q_j' q_h' dy, \quad Py_{jh}^{4,2} = \int_0^{\frac{1}{2}(1-r_b)} g^3(y) q_j' q_h' dy$$

$$Py_{jh}^{4,3} = Py_{jh}^{4,1}, \quad Py_{jh}^{4,4} = \int_{\frac{1}{2}(1+r_b)}^1 g^3(y) q_j' q_h' dy,$$

$$Ry_{jh}^1 = \int_0^1 q_j(y)q_h(y)dy, \quad Ry_{jh}^2 = Ry_{jh}^1, \quad Ry_{jh}^3 = q'_j(0)q'_h(0), \quad Ry_{jh}^4 = q'_j(1)q'_h(1)$$

$$Ty_{jh}^1 = \int_0^1 q_j(y)q_h(y)dy, \quad Ty_{jh}^2 = Ty_{jh}^1, \quad Ty_{jh}^3 = q_j(0)q_h(0), \quad Ty_{jh}^4 = q_j(1)q_h(1)$$

$$Cy_{jh}^1 = \int_0^1 g(y)q_jq_hdy, \quad Cy_{jh}^2 = \int_0^{\frac{1}{2}(1-r_b)} g(y)q_jq_hdy, \quad Cy_{jh}^3 = Cy_{jh}^1,$$

$$Cy_{jh}^4 = \int_{\frac{1}{2}(1+r_b)}^1 g(y)q_jq_hdy$$

Appendix B. Definitions of variables and parameters in Eq. (17)

$$r_a = \frac{a'}{a}, \quad r_b = \frac{b'}{b}$$

$$Px_{kl}^{1,1} = \int_0^{\frac{1}{2}(1-r_a)} f^3(x)X''_kX''_ldx, \quad Px_{kl}^{1,2} = \int_{\frac{1}{2}(1-r_a)}^{\frac{1}{2}(1+r_a)} f^3(x)X''_kX''_ldx,$$

$$Px_{kl}^{1,3} = \int_{\frac{1}{2}(1+r_a)}^1 f^3(x)X''_kX''_ldx,$$

$$Px_{kl}^{1,4} = Px_{kl}^{1,2}, \quad Px_{kl}^{2,1} = \int_0^{\frac{1}{2}(1-r_a)} f^3(x)X_kX_ldx, \quad Px_{kl}^{2,2} = \int_{\frac{1}{2}(1-r_a)}^{\frac{1}{2}(1+r_a)} f^3(x)X_kX_ldx,$$

$$Px_{kl}^{2,3} = \int_{\frac{1}{2}(1+r_a)}^1 f^3(x)X_kX_ldx, \quad Px_{kl}^{2,4} = Px_{kl}^{2,2}, \quad Px_{kl}^{31,1} = \int_0^{\frac{1}{2}(1-r_a)} f^3(x)X'_lX_kdx,$$

$$Px_{kl}^{31,2} = \int_{\frac{1}{2}(1-r_a)}^{\frac{1}{2}(1+r_a)} f^3(x)X'_lX_kdx, \quad Px_{kl}^{31,3} = \int_{\frac{1}{2}(1+r_a)}^1 f^3(x)X'_lX_kdx, \quad Px_{kl}^{31,4} = Px_{kl}^{31,2},$$

$$Px_{kl}^{32,1} = \int_0^{\frac{1}{2}(1-r_a)} f^3(x)X''_kX_ldx, \quad Px_{kl}^{32,2} = \int_{\frac{1}{2}(1-r_a)}^{\frac{1}{2}(1+r_a)} f^3(x)X''_kX_ldx,$$

$$Px_{kl}^{32,3} = \int_{\frac{1}{2}(1+r_a)}^1 f^3(x)X''_kX_ldx,$$

$$Px_{kl}^{32,4} = Px_{kl}^{32,2}, \quad Px_{kl}^{4,1} = \int_0^{\frac{1}{2}(1-r_a)} f^3(x)X'_kX'_ldx, \quad Px_{kl}^{4,2} = \int_{\frac{1}{2}(1-r_a)}^{\frac{1}{2}(1+r_a)} f^3(x)X'_kX'_ldx,$$

$$\begin{aligned}
Px_{kl}^{4,3} &= \int_{\frac{1}{2}(1+r_a)}^1 f^3(x) X_k' X_l' dx, \quad Px_{kl}^{4,4} = Px_{kl}^{4,2} \\
Rx_{kl}^1 &= X_k'(0) X_l'(0), \quad Rx_{kl}^2 = X_k'(1) X_l'(1), \quad Rx_{kl}^3 = \int_0^1 X_k X_l dx, \quad Rx_{kl}^4 = Rx_{kl}^3 \\
Tx_{kl}^1 &= X_k(0) X_l(0), \quad Tx_{kl}^2 = X_k(1) X_l(1), \quad Tx_{kl}^3 = Rx_{kl}^3, \quad Tx_{kl}^4 = Tx_{kl}^3 \\
Cx_{kl}^1 &= \int_0^{\frac{1}{2}(1-r_a)} f(x) X_k X_l dx, \quad Cx_{kl}^2 = \int_{\frac{1}{2}(1-r_a)}^{\frac{1}{2}(1+r_a)} f(x) X_k X_l dx, \\
Cx_{kl}^3 &= \int_{\frac{1}{2}(1+r_a)}^1 f(x) X_k X_l dx, \quad Cx_{kl}^4 = Cx_{kl}^2 \\
Py_{kl}^{1,1} &= \int_0^1 g^3(y) Y_k Y_l dy, \quad Py_{kl}^{1,2} = \int_0^{\frac{1}{2}(1-r_b)} g^3(y) Y_k Y_l dy, \quad Py_{kl}^{1,3} = Py_{kl}^{1,1}, \\
Py_{kl}^{1,4} &= \int_{\frac{1}{2}(1+r_b)}^1 g^3(y) Y_k Y_l dy \\
Py_{kl}^{2,1} &= \int_0^1 g^3(y) Y_k'' Y_l'' dy, \quad Py_{kl}^{2,2} = \int_0^{\frac{1}{2}(1-r_b)} g^3(y) Y_k'' Y_l'' dy, \quad Py_{kl}^{2,3} = Py_{kl}^{2,1}, \\
Py_{kl}^{2,4} &= \int_{\frac{1}{2}(1+r_b)}^1 g^3(y) Y_k'' Y_l'' dy \\
Py_{kl}^{31,1} &= \int_0^1 g^3(y) Y_k'' Y_l dy, \quad Py_{kl}^{31,2} = \int_0^{\frac{1}{2}(1-r_b)} g^3(y) Y_k'' Y_l dy, \quad Py_{kl}^{31,3} = Py_{kl}^{31,1}, \\
Py_{kl}^{31,4} &= \int_{\frac{1}{2}(1+r_b)}^1 g^3(y) Y_k'' Y_l dy \\
Py_{kl}^{32,1} &= \int_0^1 g^3(y) Y_k Y_l'' dy, \quad Py_{kl}^{32,2} = \int_0^{\frac{1}{2}(1-r_b)} g^3(y) Y_k Y_l'' dy, \quad Py_{kl}^{32,3} = Py_{kl}^{32,1}, \\
Py_{kl}^{32,4} &= \int_{\frac{1}{2}(1+r_b)}^1 g^3(y) Y_k Y_l'' dy \\
Py_{kl}^{4,1} &= \int_0^1 g^3(y) Y_k' Y_l' dy, \quad Py_{kl}^{4,2} = \int_0^{\frac{1}{2}(1-r_b)} g^3(y) Y_k' Y_l' dy, \quad Py_{kl}^{4,3} = Py_{kl}^{4,1}, \\
Py_{kl}^{4,4} &= \int_{\frac{1}{2}(1+r_b)}^1 g^3(y) Y_k' Y_l' dy \\
Ry_{kl}^1 &= \int_0^1 Y_k Y_l dy, \quad Ry_{kl}^2 = Ry_{kl}^1, \quad Ry_{kl}^3 = Y_k'(0) Y_l'(0), \quad Ry_{kl}^4 = Y_k'(1) Y_l'(1)
\end{aligned}$$

$$Ty_{kl}^1 = \int_0^1 Y_k Y_l dy, \quad Ty_{kl}^2 = Ty_{kl}^1, \quad Ty_{kl}^3 = Y_k(0)Y_l(0), \quad Ty_{kl}^4 = Y_k(1)Y_l(1)$$

$$Cy_{kl}^1 = \int_0^1 g(y)Y_k Y_l dy, \quad Cy_{kl}^2 = \int_0^{\frac{1}{2}(1-r_b)} g(y)Y_k Y_l dy, \quad Cy_{kl}^3 = Cy_{kl}^1$$

$$Cy_{kl}^4 = \int_{\frac{1}{2}(1+r_b)}^1 g(y)Y_k Y_l dy$$

References

- [1] Leissa AW. *Vibration of plates*, Nasa, SP 160, 1969.
- [2] Laura PAA, Gutierrez RH, et al. Free vibrations of rectangular plates elastically restrained against rotation with circular or square free openings. *Ocean Engng* 1987;14(4):285–93.
- [3] Laura PAA, Romanelli E, Rossi RE. Transverse vibrations of simply supported rectangular plates with rectangular cutouts. *Journal of Sound and Vibration* 1997;202(2):275–83.
- [4] Gutierrez RH, Laura PAA, Pombo JL. Higher frequencies of transverse vibration of rectangular plates elastically restrained against rotation at the edges and with a central free hole. *Journal of Sound and Vibration* 1987;117(1):202–6.
- [5] Laura PAA, Avalos DR, Larrondo HA, Rossi RE. Numerical experiments on the Rayleigh–Ritz method when applied to doubly connected plates in the case of free edge holes. *Ocean Engng* 1998;25(7):585–9.
- [6] Laura PAA, Gutierrez RH, Ercoli L, Utjes JC, Carnicer R. Free vibrations of rectangular plates elastically restrained against rotation with circular or square free openings. *Ocean Engng* 1987;14(4):285–93.
- [7] Mikhlin SG. *Variational methods in mathematical physics*. Oxford: Pergamon Press, 1964.
- [8] Bhat RB. Natural frequencies of rectangular plates using characteristic orthogonal polynomials in Rayleigh–Ritz method. *Journal of Sound and Vibration* 1985;102:493–9.
- [9] Bhat RB. Plate deflection using orthogonal polynomials. *Journal of Engineering Mechanics* 1985;101:1301–9.